Optics Communications 492 (2021) 126988

Contents lists available at ScienceDirect

Optics Communications

journal homepage: www.elsevier.com/locate/optcom

60 Gbit/s PAM-4 wireless transmission in the 310 GHz band with nonlinearity tolerant signal processing

Mengyao Qiao [a], Lu Zhang [a,b,*], Shiwei Wang [a], Wei Li [a], Zijie Lu [a], Xiaodan Pang [c], Le Zhang [d], Shilie Zheng [a], Xiaofeng Jin [a], Xianmin Zhang [a], Xianbin Yu [a,b,**]

[a] The College of Information Science and Electronic Engineering, Zhejiang University, Hangzhou 310027, China
[b] Zhejiang Lab, Hangzhou 310000, China
[c] Royal Institute of Technology, Stockholm SE-10044, Sweden
[d] China Jiliang University, Hangzhou 310018, China

ARTICLE INFO

Keywords:
THz photonics
THz communication
Direct detection
PAM-4
Volterra filtering

ABSTRACT

We experimentally demonstrate a terahertz (THz) photonic wireless transmission system in the 310 GHz band with four-level pulse amplitude modulation (PAM-4) signals. A zero-bias diode is used as a simple direct detection receiver, which is cost-effective compared to a conventional coherent receiver. Moreover, we comprehensively investigate the system performance by applying linear and nonlinear equalization schemes. The experimental results show that Volterra nonlinear filtering can significantly improve the system capacity by around 90%, and transmissions of up to 60 Gbit/s PAM-4 signals over a 3 m wireless link are successfully achieved. The advantageous features of this make it promising for high-speed THz wireless communications.

1. Introduction

Data rates in wireless communications have been increasing exponentially over the recent decades [1]. To fulfill the capacity requirements, research efforts are naturally focused on the scope of terahertz (THz, 300 GHz–10 THz) communications with plentiful bandwidth resources [2]. The implementation scheme of THz wireless communication systems can be categorized as photonic scheme [3] and pure-electronic scheme [4], while photonics-based THz transmission mechanism provides benefits, such as large modulation bandwidth and signal transparency to optical fiber networks. In recent years, plenty of high-speed photonic wireless communication systems in the THz band have been experimentally demonstrated, with data rates of tens of Gbit/s up to 300 Gbit/s in the 300–500 GHz band by using advanced modulation formats like quadrature phase shift keying (QPSK), 16-point quadrature amplitude modulation (16-QAM) [5–7]. However, the aforementioned systems necessarily require a coherent detection receiver based on frequency multiplication of an electrical local oscillator (LO) and external radio frequency (RF) mixing, which increase the receiver complexity.

As we all know, direct detection scheme requires only one diode at the receiver side, which is relatively cost-effective without any additional RF sources. In the last decade, direct detection has been explored for THz photonic wireless communication utilizing modulation formats such as non-return-to-zero [8] and duobinary [9]. It is noted that the spectral efficiency of them is not sufficient to support large capacity.

Alternatively, pulse amplitude modulation (PAM) has been widely studied as a promising candidate for high-speed optical communications because it is simple and cost-effective to improve date rates with low implementation complexity [10]. Recently, some work on pure-electronic directly detected PAM-4 systems in the sub-THz and THz region has been reported by employing simple digital equalization, for instance, 30Gbit/s 150 GHz PAM-4 wireless transmission over 5 cm with digital predistortion (DPD) [11]. While taking into account the limited obtainable THz power, any further efforts to increase the nonlinearity tolerance and to extend the wireless reach of high capacity THz PAM-4 wireless systems are appreciated.

In this paper, we experimentally demonstrated a THz PAM-4 photonic wireless transmission system operating in the 310 GHz band assisted by direct detection. Advancing the modulation order always raises an issue that a direct detection system is subject to penalties due to the nonlinear behaviors, such as the nonlinear transfer function of modulators, signal-to-signal beating interference (SSBI) from direct detectors, which must be comprehensively handled from viewpoint of improving the system performance and capacity. To compensate the nonlinear impairments in our system, we propose to employ the commonly used Volterra decision feedback equalizer (Volterra-DFE) algorithm [12]. By combining a cutting-edge uni-traveling-carrier photodiode (UTC-PD) as THz emitter and a zero-bias diode (ZBD) as THz

* Corresponding author.
** Corresponding author at: The College of Information Science and Electronic Engineering, Zhejiang University, Hangzhou 310027, China.
E-mail addresses: zhanglu1993@zju.edu.cn (L. Zhang), xyu@zju.edu.cn (X. Yu).

https://doi.org/10.1016/j.optcom.2021.126988
Received 26 June 2020; Received in revised form 7 January 2021; Accepted 29 March 2021
Available online 31 March 2021

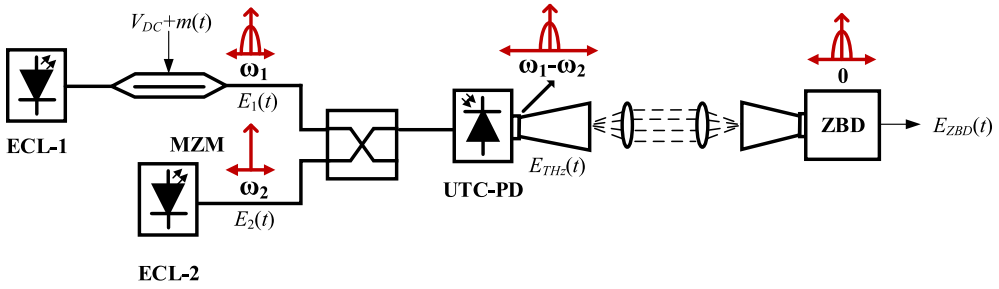

Fig. 1. Schematic diagram of the THz PAM-4 transmission system utilizing direct detection scheme.

receiver, as well as advanced digital signal processing (DSP) routine, the nonlinearity tolerance of PAM-4 systems and high speed photonic-wireless transmission performance are experimentally investigated.

2. Operational principles

2.1. Direct detection THz system

The schematic diagram of direct detection-based THz photonic-wireless transmission system is presented in Fig. 1. In this approach, THz signals are generated by the photo-mixing of two optical waves in a UTC-PD and the baseband signals are detected by a ZBD. At the transmitter, a Mach–Zehnder modulator (MZM) is used to modulate baseband signals with multi-level amplitude information. Assuming the MZM is biased at its linear region, the electrical field at the output of the MZM is given as:

$$E_1(t) = \sqrt{P_s} \cdot [aV(t) + b] \cdot \exp[j(\omega_1 t + \varphi_{n1}(t))], \tag{1}$$

where P_s, ω_1 and $\varphi_{n1}(t)$ are the power, angular frequency, and phase of an external cavity laser (ECL-1), respectively, and a, b present the modulation depth and intercept of the MZM linear region. Here $V(t)$ is the applied driving voltage:

$$V(t) = V_{DC} + m(t), \tag{2}$$

where V_{DC} is the direct current bias voltage and $m(t)$ is the driving signals, which corresponds to the PAM-4 signals here.

The optical baseband signals at the frequency of are then coupled with another optical carrier with a center frequency of from the ECL-2. This laser performs as an optical local oscillator (LO), with an electrical field expressed as:

$$E_2(t) = \sqrt{P_c} \cdot \exp[j(\omega_2 t + \varphi_{n2}(t))], \tag{3}$$

where P_c, and $\varphi_{n2}(t)$ are the power, angular frequency, and phase of the optical local oscillator. After the optical combination and heterodyne mixing at the UTC-PD, the generated THz signals can be expressed as:

$$\begin{aligned} E_{THz}(t) &= [E_1(t) + E_2(t)] \cdot [E_1(t) + E_2(t)]^* \cdot R_1 \\ &\approx 2R_1\sqrt{P_s P_c}[aV(t) + b]\cos[(\omega_1 - \omega_2)t + \varphi_{n1}(t) - \varphi_{n2}(t)], \end{aligned} \tag{4}$$

where R_1 is the responsivity of the UTC-PD. Subsequently, the THz signals are radiated into a wireless link and directly detected by the ZBD, which is a square-law based component. Taking into account the output RF bandwidth limitation of the ZBD detector, the output signals can be expressed as:

$$\begin{aligned} E_{ZBD}(t) &= E_{THz}(t) \cdot E_{THz}(t)^* \cdot R_2 \approx 2P_s P_c {R_1}^2 R_2[aV(t) + b]^2 \\ &= 4aP_s P_c {R_1}^2 R_2(aV_{DC} + b)m(t) + 2a^2 P_s P_c {R_1}^2 R_2 m^2(t) \\ &\quad + 2P_s P_c {R_1}^2 R_2(aV_{DC} + b)^2, \end{aligned} \tag{5}$$

where R_2 is the responsivity of the ZBD. It is note that in order to simply the model derivation, the channel response and impairments in the system are not considered here. As indicated in Eq. (5), the detected signals contain desired PAM-4 signals (first-term), a SSBI component (second-term) and a DC component (third-term). Apparently, the nonlinear distortions caused by SSBI would deteriorate the system performance, which needs to be further processed by DSP method at the receiver side.

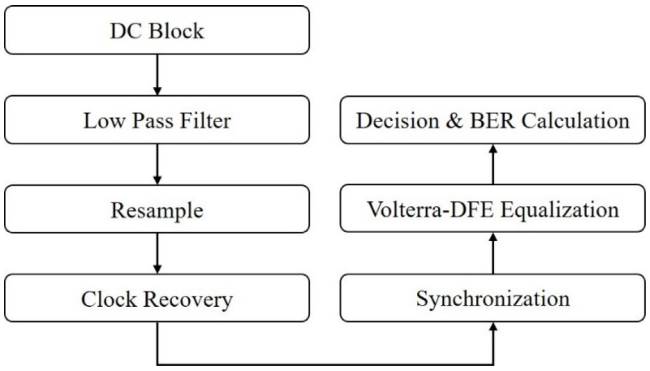

Fig. 2. The DSP routine at the receiver.

2.2. Digital signal processing routine

The proposed DSP routine at the receiver side is shown in Fig. 2. At the receiver, the signals are first captured from the oscilloscope. In the experiment, the signals sampled at 160 GSa/s are processed by MATLAB. First, the mean value of received signals is subtracted to remove the direct current (DC) component. After that, the received signals are filtered by a Gaussian lowpass filter with the bandwidth of 1.05 times of the baud rate, and the cut-off frequency of the filter is determined by the baud rate of PAM-4 signals. Afterwards, the signals are resampled to convert the sampling rate of signals from 160GSa/s to an integer times of baud rate. Then, the clock is recovered based on maximum variance-based timing recovery algorithm and generate a local clock, which matches the baud rate of the transmitted PAM-4 signals [13]. The synchronization is performed by using cross-correlation function, to find the head of the received signals.

A nonlinearity tolerant DSP algorithm based on Volterra filtering [14–16] is further employed. Here, Volterra filtering is implemented on the basis of decision feedback equalizer (DFE) scheme, and DFE is employed to mitigate the inter-symbol-interference (ISI). The equalizer can be described by the following formula:

$$\begin{aligned} y(n) &= \sum_{i=1}^{L_1} a(i)x(n - i + 1 + D_1) \\ &\quad + \sum_{i=1}^{L_2}\sum_{j=1}^{L_2} b(i,j)x(n - i + 1 + D_2)x(n - j + 1 + D_2) \\ &\quad + \sum_{i=1}^{L_3}\sum_{j=1}^{L_3}\sum_{k=1}^{L_3} c(i,j,k)x(n - i + 1 + D_3)x(n - j + 1 + D_3) \\ &\quad \times x(n - k + 1 + D_3) - \sum_{i=1}^{W} f(i)d(n - i), \end{aligned} \tag{6}$$

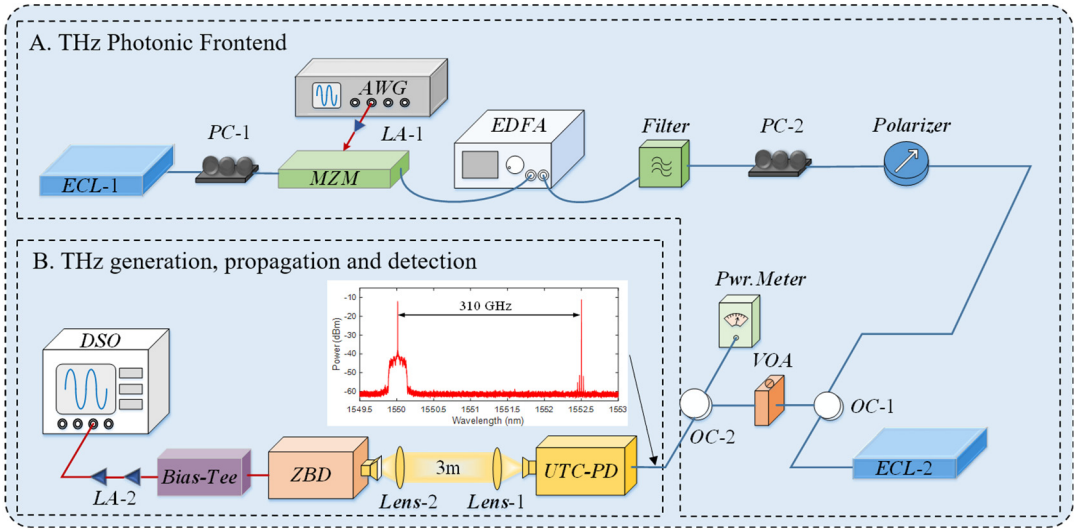

Fig. 3. Experimental setup of THz PAM-4 photonic-wireless transmission system. The inset: optical spectrum at the input of the UTC-PD with 30 Gbaud PAM-4 signal modulation. (ECL: external cavity laser, PC: polarization controller, MZM: Mach–Zehnder modulator, AWG: arbitrary waveform generator, EDFA: Erbium-doped fiber amplifier, OC: optical coupler, VOA: variable optical attenuator, UTC-PD: uni-traveling carrier photodiode, ZBD: zero-bias detector, LA: linear amplifier, DSO: digital storage oscilloscope).

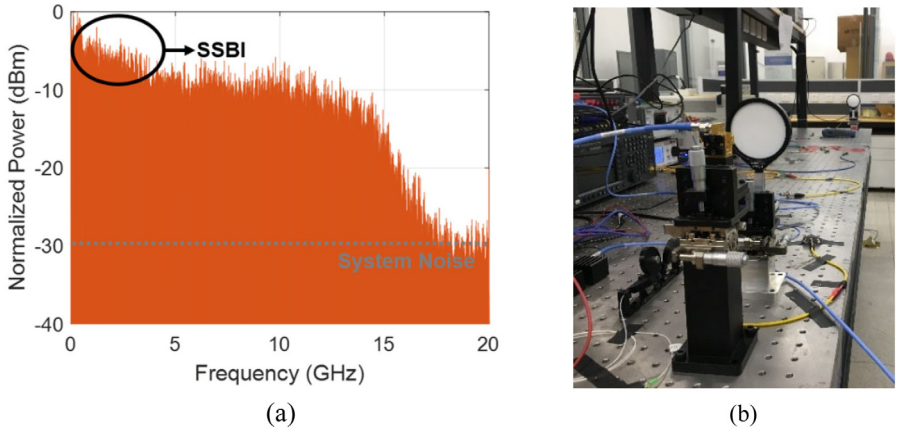

Fig. 4. (a) The electrical spectrum of the received baseband PAM-4 signal and (b) The photograph of the 3 m THz wireless link.

where $x(n)$ is the samples of the received signals, $a(i)$ is the linear equalization coefficients, $b(i, j)$ and $c(i, j, k)$ are the second-order and third-order equalization coefficients, respectively. L_1, L_2 and L_3 are the memory length of different order effects. The aforementioned terms correspond to the feed-forward section of the equalizer. In the last term, $f(i)$ is the feedback coefficients of the equalizer and W is the memory length of feedback taps, $d(n)$ is the training symbols in training period and the decision symbols in the decision period. D_1, D_2 and D_3 are the reference tap numbers of different term orders, which are used as delay factors to change the position of reference taps. The training symbols are predefined in the PAM-4 symbols at the transmitter side. The optimum equalizer coefficients are trained and obtained by the least mean squares (LMS) algorithm [17]. The optimized parameters in Volterra-DFE algorithm will be given in Section 4. Finally, the signals are recovered by decision and de-mapping modules to get the BER performance.

3. Experimental setup

Fig. 3 shows the experimental setup of THz PAM-4 photonic wireless transmission system. The setup consists of two sections presenting THz photonic frontend and THz generation, propagation and detection, respectively. In the setup, a narrow-band UTC-PD operating in the frequency range of 280–380 GHz (NTT Electronics Corp. IOD-PMJ-13001) is employed as the THz emitter, and a ZBD operating in the frequency band 220–330 GHz with a maximum response bandwidth of 40 GHz (Virginia Diode WR3.4ZBD) is used to down-convert the THz signals to the baseband. The responsivity of the ZBD is 1500 V/W. In the experiment, we use two tunable ECLs (<100 kHz linewidth) as optical sources to emit continuous-wave carriers. One optical carrier from the ECL-1 (1550.01 nm) is launched into a polarization controller (PC) to control the polarization state to an MZM (3-dB bandwidth: 25 GHz). The PAM-4 signals are derived from a pseudo random bit sequence (PRBS) with a word length of 2^{15}-1 from an arbitrary waveform generator (AWG, Keysight M8195 A, 65 GSa/s sampling rate, 25 GHz analog bandwidth). The baseband signals are amplified by an Erbium-doped fiber amplifier (EDFA) and filtered by an optical band-pass filter to suppress the out-of-band amplified spontaneous emission noise. As polarization aligned by a polarizer controller (PC) and a polarizer, the baseband signals are power balanced with the free-running LO ECL-2. The LO ECL-2 is centered at 1552.5 nm with output power of 15.3 dBm and combined with the baseband signals using a 3-dB optical coupler (OC-1), resulting in a wavelength difference of 310 GHz. The coupled optical signals are finally sent into an UTC-PD for photo-mixing generation of THz signals. As an example, the combined optical spectrum of two-wavelength with 30 Gbaud PAM4 signals is shown in the inset of Fig. 3. When the optical power into UTC-PD is 14 dBm, the

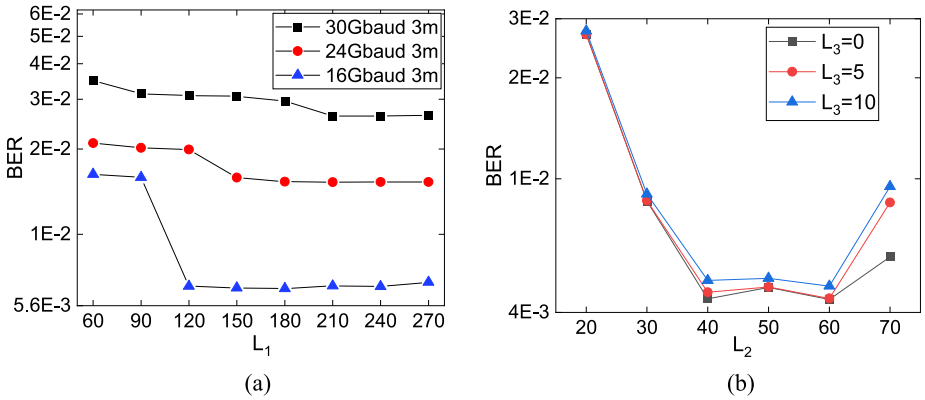

Fig. 5. Measured BER performance as a function of (a) the tap length L_1 of linear equalizer coefficients at different baud rates, (b) the tap length of second-order and third-order coefficients, L_2 and L_3.

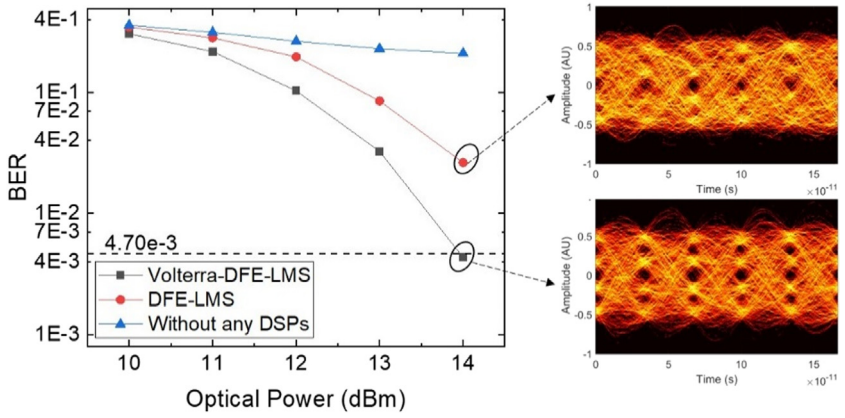

Fig. 6. The measured BER performance of PAM-4 signals after 3 m wireless transmission using DFE-LMS, Volterra-DFE and no DSP algorithms as well as eye diagrams at 14 dBm optical power.

output power of the THz signals is -11 dBm. The THz signals are then emitted by a horn antenna (25dBi gain) and radiated into a 3 m wireless link with a pair of lenses to collimate the THz beam. At the receiver, the THz signals are received by a horn antenna (25dBi gain). A ZBD and a bias-tee are used to recover the baseband PAM-4 signals. The output signals are then amplified by two linear amplifiers (SHF S804B, 22 dB gain) and analog-to-digital converted by using a broadband real-time digital sampling oscilloscope (DSO, Keysight DSOZ594 A, 160 GSa/s sampling rate, 59 GHz analog bandwidth) for further digital signal processing.

Fig. 4(a) and Fig. 4(b) shows the electrical spectrum of the received baseband signals of 60 Gbit/s PAM-4 signals and the photograph of the 3 m THz wireless link. The SSBI effect is severe in the system. Moreover, the saturation effect of electrical amplifiers will also cause nonlinear impairments. The transmission performance improvements with the nonlinear equalizer will be shown in the next section.

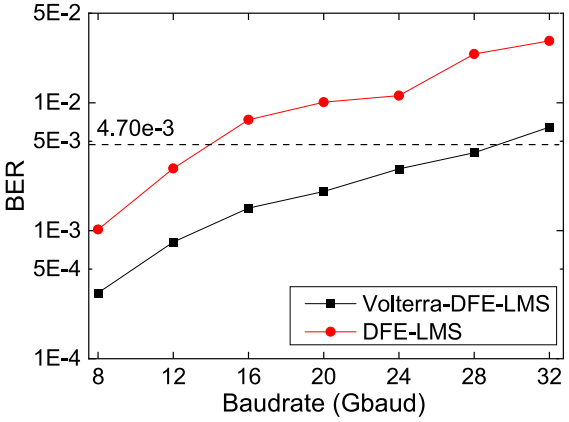

Fig. 7. The BER performance after 3 m wireless transmission using DFE-LMS and Volterra-DFE algorithms as a function of baud rate.

4. Results and discussions

The transmission performance of PAM-4 signals after the 3 m wireless link is first investigated to optimize the linear kernel of Volterra DFE algorithm. In the experiment, the optimization of the reference tap numbers is carried out by the LMS algorithm and D_1, D_2 and D_3 are set to 4. We compare the BER performance at different baud rates by altering the memory length of linear equalizer coefficients L_1 in the DFE algorithm, while the optical power of UTC-PD is kept as 14 dBm. As shown in Fig. 5(a), the optimal L_1 generally varies with the baud rates, and the higher baud rates are, the larger L_1 is required. In the following experiment, L_1 is set as 210 to guarantee optimized transmission performance. In the experiment, BER changes very little with different memory length of feedback taps W. Thus, W is set to 5 to reduce the complexity. Then we optimize the BER performance of 30 Gbaud PAM-4 signals using the Volterra-DFE algorithm with LMS. The performance is examined by estimating the dependence of L_2 and L_3 in Eq. (6). As shown in Fig. 5(b), we can observe that the best BER performance is achieved when L_2 is ranging from 40 to 60 for all cases with different L_3. Because of overfitting from the far past samples, the BER is increased again when L_2 is larger than 60. In order to

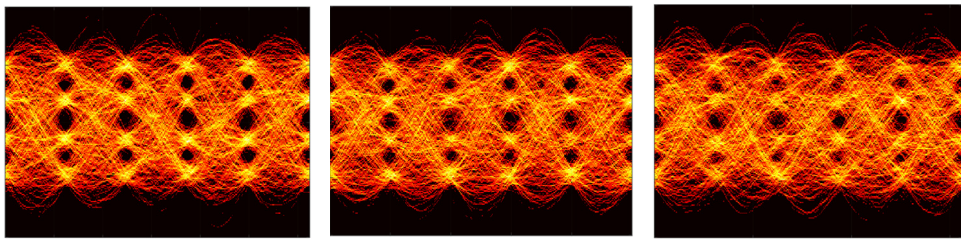

Fig. 8. Eye diagrams at (a) 8 Gbaud, (b) 20 Gbaud, (c) 32 Gbaud based on Volterra-DFE equalization.

reduce computational complexity, L_2 is set to 40. Besides, the measured BER in Fig. 5(b) exhibits approximately the same performance with different memory length of the third-order coefficients, indicating that the second-order equalizer is sufficient to compensate the nonlinearity in our experiment. These results also confirm the analysis in Eq. (5), where the nonlinear SSBI is dominant in the nonlinear system impairments. Therefore, the third-order and higher-order nonlinear terms in the Volterra series can be negligible to decrease the computational complexity.

Based on the aforementioned parameters, the measured BER performance of 30 Gbaud PAM-4 signals after 3 m wireless transmission with DFE-LMS algorithm, Volterra-DFE algorithm and without any DSP algorithms are shown in Fig. 6. When the optical power into UTC-PD reaches 14 dBm, the output THz signal power of UTC-PD is -11 dBm and eye diagrams with different algorithms are shown in Fig. 6. We can observe that the BER performance gets better with the increasing of optical power. When the optical power into UTC-PD is 14 dBm, the BER reaches 4.35e−3, which is below the hard decision forward-error-correction (HD-FEC) threshold of 4.7e−3 [18], resulting in a net rate of 56.47 Gbit/s in the 310 GHz band after paying the FEC overhead of 6.25% [18].

Fig. 7 presents the BER performance at different baud rates when optical power into UTC-PD is 14 dBm, by applying DFE-LMS and Volterra-DFE algorithms. The limitation of achieved data rates in this work is the available bandwidth of the UTC-PD and ZBD as well as low signal-to-noise ratio (SNR) due to the low THz signal power. With the increase of the baud rates, SNR decreases and the BER performance becomes worse. The Volterra-DFE based nonlinear equalization can significantly enhance the system capacity compared to DFE-based linear equalization. The experimental results indicate almost 90% baud rate enhancement, from around 16 Gbaud with DFE equalization to 30 Gbaud with Volterra-DFE equalization. The obtained eye diagrams at different baud rates based on Volterra-DFE equalization are shown in Fig. 8. When the input optical power reaches 14 dBm, the BER values of 8 Gbaud, 20 Gbaud and 32 Gbaud cases are 3.26e−4, 2.02e−3 and 6.42e−3, respectively.

5. Conclusions

We have experimentally demonstrated a THz wireless communication system in the 310 GHz band delivering up to 30 Gbaud PAM-4 signals over a 3 m THz wireless link. The employment of PAM-4 modulation enables the simplification of system architecture, allowing the use of ZBD as a cost-effective THz direct detection receiver. Moreover, by using the Volterra-DFE algorithm at the receiver side to compensate the nonlinearity impairments and ISI in the photonic wireless system, the system nonlinearity tolerance and capacity are significantly improved. The proposed system has a great potential for use in future high-speed wireless communications.

Declaration of competing interest

The authors declare that they have no known competing financial interests or personal relationships that could have appeared to influence the work reported in this paper.

Acknowledgments

The work is supported by the Swedish Research Council (VR) Starting Grant 2019–05197, and the Fundamental Research Funds for the Central Universities, China 2020QNA5012, the National Key Research and Development Program of China (Grants no. 2020YFB1805704, 2018YFB1801500 & 2018YFB2201700), the National Natural Science Fund Foundation of China under Grants 61771424 and 61871345, and in part by the Natural Science Foundation of Zhejiang Province, China under Grant LZ18F010001. The authors would like to thank the training platform of information and microelectronic engineering from the Polytechnic Institute in Zhejiang University.

References

[1] S. Koenig, D. Lopez-Diaz, J. Antes, F. Boes, R. Henneberger, A. Leuther, A. Tessmann, R. Schmogrow, D. Hillerkuss, R. Palmer, T. Zwick, C. Koos, W. Freude, O. Ambacher, J. Leuthold, I. Kallfass, Wireless sub-THz communication system with high data rate, Nature Photon. 7 (2013) 977–981.

[2] X. Yu, Y. Chen, M. Galili, T. Morioka, P.U. Jepsen, L.K. Oxenløwe, The prospects of ultra-broadband THz wireless communications, in: Proc. Int. Conf. Transparent Opt. Netw., 2014.

[3] T. Nagatsuma, G. Ducournau, C.C. Renaud, Advances in terahertz communications accelerated by photonics, Nature Photon. 10 (2016) 371–379.

[4] I. Kallfass, I. Dan, S. Rey, P. Harati, J. Antes, A. Tessmann, S. Wagner, M. Kuri, R. Weber, H. Massler, A. Leuther, T. Merkle, T. Kürner, Towards MMIC-based 300 GHz indoor wireless communication systems, in: IEICE Transactions on Electronics E98-C, 2015, pp. 1081–1090.

[5] K. Liu, S. Jia, S. Wang, X. Pang, W. Li, S. Zheng, H. Chi, X. Jin, X. Zhang, X. Yu, 100 Gbit/s THz photonic wireless transmission in the 350-GHz band with extended reach, IEEE Photonics Technol. Lett. 30 (2018) 1064–1067.

[6] X. Pang, S. Jia, O. Ozolins, X. Yu, H. Hu, L. Marcon, P. Guan, F. Da Ros, S. Popov, G. Jacobsen, M. Galili, T. Morioka, D. Zibar, L.K. Oxenløwe, 260 Gbit/s photonic-wireless link in the THz band, in: Proc. IEEE Photonics Conf., 2016.

[7] X. Li, J. Yu, L. Zhao, W. Zhou, K. Wang, M. Kong, G.K. Chang, Y. Zhang, X. Pan, X. Xin, 132-Gb/s photonics-aided single-carrier wireless terahertz-wave signal transmission at 450 GHz enabled by 64 QAM modulation and probabilistic shaping, in: Optical Fiber Communications Conference (2019) M4F. 4.

[8] T. Nagatsuma, G. Carpintero, Recent progress and future prospect of photonics-enabled terahertz communications research, IEICE Trans. Electron. 98 (2015) 1060–1070.

[9] L. Moeller, J. Federici, K. Su, THz Wireless Communications: 2.5 Gb/S Error-Free Transmission At 625 GHz using a Narrow-Bandwidth 1 MW THz Source, in: URSI General Assembly and Scientific Symposium, 2011.

[10] K. Zhong, W. Chen, Q. Sui, J. Man, A. Lau, C. Lu, L. Zeng, Experimental Demonstration of 500Gbit/s Short Reach Transmission Employing PAM4 Signal and Direct Detection with 25Gbps Device, in: Optical Fiber Communication Conference, 2015.

[11] Y. Kim, B. Hu, R. Huang, et al., 150-GHz CMOS TX/RX with digitally predistorted PAM-4 modulation for terahertz contactless/plastic waveguide communications, IEEE Trans. Terahertz Sci. Technol. 10 (2020) 370–382.

[12] G. Stepniak, J. Siuzdak, P. Zwierko, Compensation of a VLC phosphorescent white LED nonlinearity by means of Volterra DFE, IEEE Photon. Technol. Lett. 25 (2013) 1597–1600.

[13] X. Pang, J.V. Kerrebrouck, O. Ozolins, R. Lin, A. Udalcovs, L. Zhang, S. Spiga, M.C. Amann, G.V. Steenberge, L. Gan, M. Tang, S. Fu, R. Schatz, G. Jacobsen, S. Popov, D. Liu, W. Tong, G. Torfs, J. Bauwelinck, X. Yin, J. Chen, 7×100 Gbps PAM-4 Transmission over 1-km and 10-km Single Mode 7-core Fiber using 1.5-μm SM-VCSEL, in: Optical Fiber Communications Conference (2018) M1I.4.

[14] L. Zhang, X. Hong, X. Pang, O. Ozolins, A. Udalcovs, R. Schatz, C. Guo, J. Zhang, F. Nordwall, K.M. Engenhardt, U. Westergren, S. Popov, G. Jacobsen, S. Xiao, W. Hu, J. Chen, Nonlinearity-aware 200 Gbit/s DMT transmission for C-band short-reach optical interconnects with a single packaged electro-absorption modulated laser, Opt. Lett. 43 (2018) 182–185.

[15] L. Agarossi, S. Bellini, F. Bregoli, P. Migliorati, Equalization of non-linear optical channels, in: Proc. IEEE Int. Conf. Commun., 1998, pp. 662–667.

[16] A. Zhu, P.J. Draxler, J.J. Yan, T.J. Brazil, D.F. Kimball, P.M. Asbeck, Open-loop digital predistorter for RF power amplifiers using dynamic deviation reduction-based volterra series, IEEE Trans. Microw. Theory Technol. 56 (2008) 1524–1533.

[17] K. Zhong, X. Zhou, J. Huo, C. Yu, C. Lu, A.P.T. Lau, Digital signal processing for short-reach optical communications: A review of current technologies and future trends, J. Lightw. Technol. 36 (2018) 377–400.

[18] L.M. Zhang, F.R. Kschischang, Staircase codes with 6% to 33% overhead, J. Lightw. Technol. 32 (2014) 1999–2002.